

## Structure of the Hamiltonian of mean force

Phillip C. Burke<sup>1,2,3</sup>, Goran Nakerst<sup>4</sup>, and Masudul Haque<sup>4</sup>

<sup>1</sup>*School of Physics, University College Dublin, Belfield, Dublin 4, Ireland*

<sup>2</sup>*Centre for Quantum Engineering, Science, and Technology, University College Dublin, Dublin 4, Ireland*

<sup>3</sup>*Department of Theoretical Physics, Maynooth University, Maynooth, Kildare, W23 F2H6, Ireland*

<sup>4</sup>*Institut für Theoretische Physik, Technische Universität Dresden, 01062 Dresden, Germany*



(Received 4 December 2023; revised 15 April 2024; accepted 6 June 2024; published 3 July 2024)

The Hamiltonian of mean force is an effective Hamiltonian that allows a quantum system, nonweakly coupled to an environment, to be written in an effective Gibbs state. We present results on the structure of the Hamiltonian of mean force in extended quantum systems with local interactions. We show that its spatial structure exhibits a “skin effect”—its difference from the system Hamiltonian dies off exponentially with distance from the system-environment boundary. For spin systems, we identify the terms that can appear in the Hamiltonian of mean force at different orders in the inverse temperature.

DOI: [10.1103/PhysRevE.110.014111](https://doi.org/10.1103/PhysRevE.110.014111)

### I. INTRODUCTION

The assumption of weak system-bath coupling is widespread in thermodynamics but is clearly not universally valid. There is thus considerable interest in formulating thermodynamics to include effects of nonweak coupling [1]. A central concept in this effort is that of the Hamiltonian of mean force (HMF) [2,3], the quantum counterpart to the classical potential of mean force [4–6]. Consider a combined system in thermal equilibrium, composed of a system  $A$  and a bath/environment  $B$ , interacting via the Hamiltonian  $H_{AB}$  so that the combined Hamiltonian is  $H = H_A + H_B + H_{AB}$ . The system state  $\rho_A$ , obtained by tracing out  $B$  degrees of freedom, is then not a thermal Gibbs state in general and differs from  $e^{-\beta H_A}$  [7–9]; here  $\beta$  is the inverse temperature. Nevertheless, we can formally define an effective Hamiltonian  $H_A^*$  so that  $\rho_A \propto e^{-\beta H_A^*}$  [10–18]. This  $H_A^*$  is the HMF. For non-negligible coupling  $H_{AB}$ , the HMF will generally deviate from the actual system Hamiltonian  $H_A$ . For extended systems with local degrees of freedom, we address the question of how  $H_A^*$  differs from  $H_A$ , in particular, the spatial dependence of this difference.

The HMF often appears implicitly in the study of thermalization in isolated quantum systems [19–25]. Any spatial segment of an isolated system ( $A$ ) can be regarded as being thermalized by the rest of the system ( $B$ ), so that the expectation values of local observables having support in  $A$  are given by their expectation values in the reduced thermal state. Since the partition between  $A$  and  $B$  is arbitrary in this setup, the coupling  $H_{AB}$  is not small, and thus the thermal state to be used is  $\rho_A \propto \text{tr}_B e^{-\beta H} \propto e^{-\beta H_A^*}$  rather than just  $e^{-\beta H_A}$ . In this context, the temperature  $1/\beta$  is determined using the canonical-ensemble correspondence between energy and temperature [19,20,22,24,26–41]. The relevance of the HMF concept in this setup raises the question of the structure of the HMF in systems with local interactions. Two questions immediately arise: (i) What is the spatial structure of the HMF, i.e., of the deviation of  $H_A^*$  from  $H_A$ ? (ii) What type of interactions are contained in the HMF?

We find that when  $\beta$  is not very large, the difference of coefficients of HMF terms from the corresponding  $H_A$  coefficients decay exponentially with distance  $d$  to the boundary between  $A$  and  $B$ , as illustrated in Fig. 1(b). This result implies a “skin effect,” illustrated in Fig. 1(a): The HMF effectively only deviates from  $H_A$  near the boundary, i.e., the “bath”  $B$  has a very shallow influence in  $A$ . This is a general result, provided the total system Hamiltonian is made of local terms. For  $\beta \rightarrow \infty$  (very low temperature), we show how the HMF is related to the “entanglement Hamiltonian” [42–45] which is calculated from the ground state alone. We formulate our results in terms of spin chains, which are paradigm models for extended quantum systems with local interactions. Using a perturbative framework coupled with numerical analysis, we elucidate the types of terms that can appear in the HMF and present systematics on which types of terms can appear at which order in  $\beta$ .

### II. DEFINITIONS & SETUP

The combined system is taken to be in a thermal state  $\rho = e^{-\beta H}/Z$ , so that subsystem  $A$  (the “system”) is in state  $\rho_A = \frac{1}{Z} \text{tr}_B e^{-\beta H}$ , where  $\text{tr}_B$  is the partial trace over  $B$ . The HMF  $H_A^*$  is defined to satisfy [2]

$$\rho_A = \frac{1}{Z^*(\beta)} e^{-\beta H_A^*(\beta)}. \quad (1)$$

This essentially defines the HMF only up to a constant [46–48]. As this freedom is not of interest to us (it only adds an identity operator to the HMF), we remove the ambiguity by choosing the normalization to be  $Z^*(\beta) = Z(\beta)/Z_B(\beta)$ , where  $Z$  and  $Z_B$  are the partition functions of the combined system and the subsystem  $B$  (“bath”), respectively. With this definition, the HMF is

$$H_A^*(\beta) = -\frac{1}{\beta} \ln \frac{\text{tr}_B(e^{-\beta H})}{\text{tr}_B(e^{-\beta H_B})}. \quad (2)$$

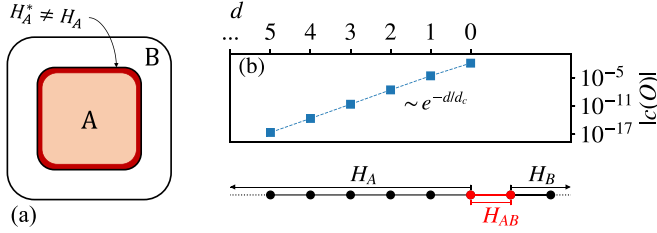


FIG. 1. (a) Illustration of the skin effect in a composite system. The dark red region indicates the shallow effect of  $B$  within  $A$ . (b) Magnitude of coefficients in the HMF plotted versus the distance  $d$  from the boundary site  $L_A$  at small  $\beta$ , illustrating the exponential decay with distance  $d$ .

The HMF  $H_A^*$  reduces to the bare system Hamiltonian  $H_A$  for vanishing coupling ( $H_{AB} = 0$ ) [49–51] and for infinite temperature ( $\beta = 0$ ) [13].

For definiteness, we formulate our results for the  $XXZ$  chain, with and without magnetic fields. This exemplifies the case of operators being supported on nearest-neighbor sites (spin-spin interactions) or single sites (magnetic fields). Generalization to longer-range interactions and to fermionic or bosonic systems should be straightforward, but we do not attempt to write out explicitly all such cases. The Hamiltonian is

$$H = J \sum_{j=1}^{L-1} (\sigma_j^x \sigma_{j+1}^x + \sigma_j^y \sigma_{j+1}^y) + \Delta \sum_{j=1}^{L-1} \sigma_j^z \sigma_{j+1}^z + \sum_{j=1}^L (h_j^z \sigma_j^z + h_j^x \sigma_j^x), \quad (3)$$

where  $J$  is the site-to-site “hopping” strength,  $\Delta$  is the spin-spin interaction strength (anisotropy), and  $h_j^z$ , ( $h_j^x$ ) denotes the strength of the onsite magnetic field in the  $z$  direction ( $x$  direction) onsite  $j$ . Unless otherwise stated, we will generally use uniform magnetic fields, i.e.,  $h_j^z = h^z$  and  $h_j^x = h^x$ ,  $\forall j$ . The case of  $h_j^x = h_j^z = 0$  is the standard  $XXZ$  chain. We take the first  $L_A$  sites as subsystem  $A$ ; the boundary bond connects sites  $j = L_A$  and  $j = L_A + 1$ .

A convenient basis to investigate the HMF of spin systems is the basis of Pauli operators. The Pauli operators  $O = \sigma_{i_1}^{\alpha_1} \dots \sigma_{i_{L_A}}^{\alpha_{L_A}}$ , where  $\alpha_j = \{x, y, z\}$  and  $i_j$  denote sites in  $A$ , together with the identity operator, form an orthogonal basis of operators with respect to the Hilbert-Schmidt scalar product. The coefficient of an operator in a Hamiltonian is given by the scalar product of the operator with the Hamiltonian. Thus, we quantify the deviation of the HMF from  $H_A$  by

$$c(O) = \text{tr}[O \cdot (H_A^*(\beta) - H_A)], \quad (4)$$

i.e., by the difference of coefficients of the same operator in the HMF and  $H_A$ .

All numerical results in this work are obtained via exact diagonalization, i.e., the canonical density matrix of the entire  $A + B$  system is constructed explicitly as a  $2^L \times 2^L$  matrix, and then the  $B$  degrees of freedom are traced out numerically. The computations are performed with 128-bit precision. This higher precision is necessary because in many cases the

TABLE I. One- and two-body terms appearing in  $H_A^*$ , for various system Hamiltonians  $H$ . The final row indicates the minimum order in  $\beta$  at which the terms can appear.

$H$	$\sigma_j^\alpha$	$\sigma_j^\alpha \sigma_{j+1}^\alpha$	$\sigma_j^\alpha \sigma_k^\alpha$	$\sigma_j^\alpha \sigma_k^{\alpha'}$
$XX$ ( $\Delta = 0$ )	.	✓	.	.
$XXZ$ ( $\Delta \neq 0$ )	.	✓	✓	.
$XXZ + \sigma_n^\alpha$	✓	✓	✓	✓
Min. order in $\beta$	$\beta^{2d+1}$	$\beta^{2d}$	$\beta^{2d}$	$\beta^{2d+1}$

coefficients are orders of magnitude smaller than the precision of double-precision floating-point arithmetic ( $\sim 10^{-16}$ ).

We refer to the  $B$  partition (sites  $L_A + 1$  to  $L$ ) as the “bath.” However, in the present setting, we are not interested in the thermalizing effect of the bath, since the full  $A + B$  system is already imposed to be in a Gibbs (thermal) state. This means that the  $B$  partition is not required to have any of the properties (zero memory, fast timescales, infinite bandwidth, etc.) that a physical bath is usually assumed to have. In particular, the  $B$  partition is not required to be larger than the  $A$  partition. In fact, we find that the size of the “bath” does not affect the qualitative insights presented in this work. Therefore, it is computationally advantageous to take the  $B$  partition to be as small as meaningful, and we present much of our data for systems with  $L = L_A + 1$ , i.e., a single site in  $B$ . This might appear to contradict the usual idea of a physical bath that thermalizes a system and sets the temperature, for which a large size is necessary or at least helpful. However, in the present setting, a single-site “bath” is perfectly reasonable.

### III. WHICH TERMS APPEAR?

Terms appearing in  $H_A^*$ , beyond those already in  $H_A$ , are formed by combining terms in  $H$ , as can be seen by considering an expansion of Eq. (2) in  $\beta$ . Thus any term in  $H_A^*$  must have the form  $O \equiv h_1 \dots h_k$  (equality up to a constant), with the  $h_i$  being terms that appear in  $H$ .

The type of Pauli operators appearing in  $H$  constrains the types that can appear in  $H_A^*$ . We outline the cases of an  $XXZ$  chain—other cases can be worked out analogously. For the  $XXZ$  Hamiltonian *without* magnetic fields, the operators appearing in the HMF can be identified by considering a homomorphism of the Klein four-group, the group of Pauli matrices modulo phases [52]. The homomorphisms are given by assigning a sign  $\pm 1$  to single-body Pauli operators  $\sigma^x$ ,  $\sigma^y$ , and  $\sigma^z$ . All terms in the  $XXZ$  Hamiltonian without magnetic fields have sign  $+1$ , regardless of the sign function. This carries over to the corresponding HMF [52]. For single-body and mixed two-body ( $\sigma_i^\alpha \sigma_j^{\alpha'}$  for  $\alpha \neq \alpha'$ ) Pauli operators, there are sign functions such that the sign of the operators is negative. Thus, these Pauli operators do not appear in the HMF. This purely algebraic argument [52] is independent of the temperature and the lattice geometry.

The  $XXZ$  Hamiltonian with magnetic fields contains single-body Pauli operators and the above argument breaks down. The corresponding HMF overlaps with all Pauli operators for any  $\beta > 0$ . In Table I, we list the one- and two-body terms that can arise in the HMF for several system Hamiltonians.

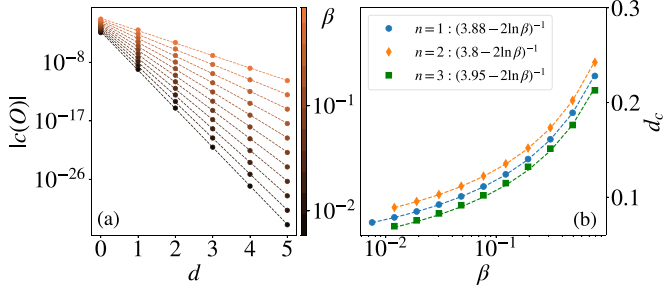


FIG. 2. (a)  $|c(O)|$  for one-body term  $\sigma_j^x$  in the HMF versus distance for various  $\beta$  (color bar). Corresponding curves for two- or three-body terms are similar [52]. (b) Skin depth  $d_c$  as function of  $\beta$ , for one-body, two-body ( $\sigma_\ell^\alpha \sigma_m^\alpha$ ), and three-body ( $\sigma_\ell^\alpha \sigma_m^\alpha \sigma_n^\alpha$ ) terms.  $n = 1$  corresponds to slopes in (a). Dashed lines are  $(a - 2 \ln \beta)^{-1}$  for fitted  $a$  (legend) for each  $n$ —shifted up/down by  $10^{-2}$  for clarity. Data for a uniform field XXZ chain with  $L = 7$ ,  $L_A = 6$ ,  $J = 1$ ,  $\Delta = 0.95$ , and  $h_x = h_z = 0.2$ .

#### IV. SMALL $\beta$

For  $\beta \rightarrow 0$ , the HMF converges to  $H_A$  [11,13]. For small  $\beta > 0$ , we find that  $H_A^*$  differs from  $H_A$  most notably close to the boundary of  $A$  with the bath  $B$ , i.e.,  $|c(O)|$  is larger for operators  $O$  supported close to the boundary than for  $O$  supported far away from the boundary. We define the distance  $d(O)$  as the distance from the boundary to the farthest site within the support of  $O$ , i.e., for an  $n$ -body Pauli operator  $O = \sigma_{i_1}^{\alpha_1} \dots \sigma_{i_n}^{\alpha_n}$  with  $i_1 < \dots < i_n$ , we have  $d(O) = L_A - i_1$ .

Remarkably,  $|c(O)|$  decays exponentially with distance  $d$  from the boundary. For one-body ( $n = 1$ ) terms, the clear exponential behavior is seen in Fig. 1(b) and Fig. 2(a); similar exponential behaviors are observed for  $n = 2$  and  $n = 3$  operators [52]. This exponential decay with distance means that the HMF differs from the bare subsystem Hamiltonian  $H_A$  only by a skin effect. The skin depth  $d_c$  is defined by

$$|c(O)| \sim e^{-d/d_c}. \quad (5)$$

The skin depth is the slope in Fig. 1(b) and Fig. 2(a). The skin depth as a function of  $\beta$  is shown for one-, two-, and three-body terms in Fig. 2(b). This dependence is very well approximated by

$$d_c \approx \frac{1}{a - 2 \ln \beta}. \quad (6)$$

The quantity  $a(O)$  is numerically found to be either independent of or at most weakly dependent on  $\beta$  and to depend on the operator  $O$ . The term  $2 \ln \beta$  is independent of the operator; we will provide a perturbative argument below.

##### A. Perturbative considerations

Equations (5) and (6) can be justified by a perturbative argument in  $\beta$ . We expand the HMF in a formal power series in  $\beta$ :

$$H_A^* = \sum_{k=0}^{\infty} \beta^k H_{A,k}^*, \quad (7)$$

with the matrix-valued coefficients [52]

$$H_{A,k-1}^* = (-1)^{k-1} \sum_{m=1}^k \frac{(-1)^{m+1}}{m D_B^m} \times \sum_{\{n_1+\dots+n_m=k\}} \left( \prod_{i=1}^m \frac{\text{tr}_B(H^{n_i})}{n_i!} \right) - [H \leftrightarrow H_B], \quad (8)$$

where the second term,  $[H \leftrightarrow H_B]$ , is obtained from the first term by replacing  $H$  with  $H_B$ .

We note that an expansion in a “unitful” quantity  $\beta$  is questionable, and indeed the expansion in Eq. (7) should be in  $\beta/J$  as the dominating scale in the Hamiltonian is  $J$ , provided  $h_j$  and  $\Delta$  are not significantly larger than  $J$ . In all numerical results, we have chosen  $J = 1$ , and thus for ease of readability we have opted to omit factors of  $J$ .

When the operators in  $H$  are traceless, the first few coefficients are [52]

$$H_{A,0}^* = H_A, \quad (9)$$

$$H_{A,1}^* = \frac{1}{2D_B} \text{tr}_B(H_{AB}^2), \quad (10)$$

$$H_{A,2}^* = \frac{1}{6D_B} [\text{tr}_B(H_{AB}H_AH_{AB}) - \text{tr}_B(H_{AB}^2)H_A]. \quad (11)$$

From Eq. (9) one infers the known result  $H_A^*(\beta) \rightarrow H_A$  for  $\beta \rightarrow 0$  [11,13], which is illustrated in Figs. 4(a) and 4(c).

We denote the overlap of operators  $O$  with  $H_{A,k}^*$  by  $c_k(O) = \text{tr}(OH_{A,k}^*)$ , and the smallest  $k \geq 1$  such that  $c_k(O)$  is nonzero by  $k_0$ . We observed that  $k_0$  is lower bounded by

$$k_0 \geq 2(d+1) - n \quad (12)$$

for  $n$ -body operators. In other words, the minimum order at which  $c(O)$  can appear is  $\mathcal{O}(\beta^{2(d+1)-n})$ . Some examples are listed in Table I.

In Figs. 3(a) and 3(b) we present  $|c(O)|$  as a function of  $\beta$  for  $n = 1$  and  $n = 2$  operators. For small  $\beta$ , the dependence is a power law with exponent  $2d + 1$  for one-body operators and  $2d$  for two-body operators  $O$  (dashed line). Similarly, we find that  $c(O)$  is of order  $\mathcal{O}(\beta^{2d-1})$  for three-body and  $\mathcal{O}(\beta^{2d-2})$  for four-body operators [52]. In addition to these examples obeying the equality in Eq. (12), we also have cases where  $k_0$  is larger than the lower bound: for mixed two-body operators  $\sigma_j^\alpha \sigma_\ell^{\alpha'}$  with  $\alpha \neq \alpha'$ ,  $c(O)$  follows a power law in  $\beta$  with exponent  $2d + 1$  ( $2d + 2$  if  $\ell = L_A$ ) [52].

Before justifying the lower bound, Eq. (12), we first highlight a consequence. We denote  $k_0 = 2d + b$ , where  $b$  is an integer, independent of  $d$  and  $\beta$ . Then

$$c(O) = e^{2d \ln \beta} \sum_{k=b}^{\infty} c_{k+2d} \beta^k. \quad (13)$$

We write the  $d$  dependence of the second factor as  $|\sum_{k=b}^{\infty} c_{k+2d} \beta^k| \sim e^{-ad}$ , where  $a$  is a real number; we assume that there is no faster dependence on  $d$ . (The prefactor may have polynomial dependence.) Then the exponential dependence of  $|c(O)|$  on  $d$  is given by

$$|c(O)| \sim e^{-(a-2 \ln \beta)d}. \quad (14)$$

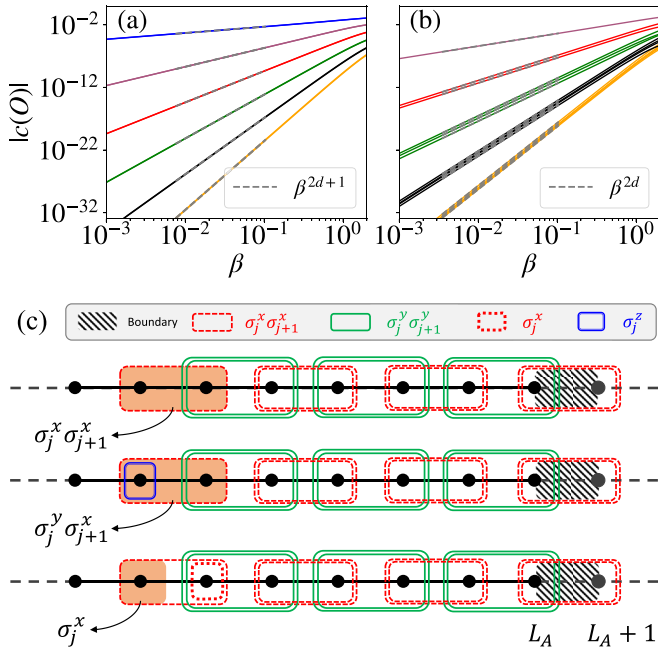


FIG. 3.  $|c(O)|$  for (a) one-body ( $\sigma_j^{(x,z)}$ ) and (b) two-body ( $\sigma_j^x \sigma_k^x$ ) operators in  $H_A^*$  versus  $\beta$ -uniform field XXZ chain with  $L = 7$ ,  $L_A = 6$ ,  $J = 1$ ,  $\Delta = 0.95$ ,  $h_x = h_z = 0.2$ . Similar results are observed in an XXZ chain with disordered fields [52]. Lines are grouped into colors representing the distance to the boundary, the top group being closest to the boundary. (c) Illustration of analytical argument for the factor of  $2d$ . Rectangles denote Pauli operators ( $h_i$ ) in  $H$ . The different colored patterns correspond to  $x, y, z$ , and the enclosed black dots indicate the support of the operator on the chain. Double rectangles mean that the operators appear twice. The orange-shaded regions indicate support of operators corresponding to the product of all Pauli operators in the string ( $O \equiv h_1, \dots, h_{k+1}$ ).

Extracting  $d_c$  from Eq. (14) implies Eq. (6). For small  $\beta$ , retaining only the first term in the sum in Eq. (13), we see that  $a$  is independent of  $\beta$  for small  $\beta$  [52]. Numerically [Fig. 2(b)],  $a$  appears to be  $\beta$ -independent at all  $\beta$ .

### B. Justification of the lower bound Eq. (12)

Equation (12) is consistent with the lowest-order expressions, Eqs. (9)–(11). By Eq. (12), two-body Pauli operators

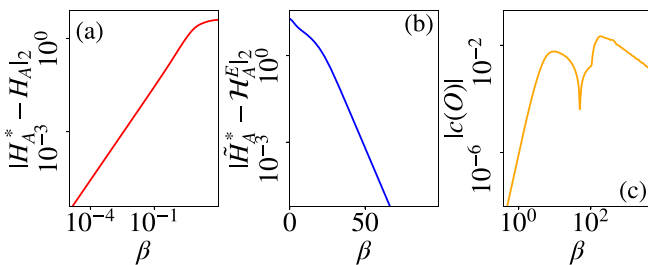


FIG. 4. Hilbert-Schmidt norm of the difference between (a)  $H_A$  and  $H_A^*$ , (b)  $\mathcal{H}_A^E$  and  $\hat{H}_A^*$ , for a uniform field XXZ chain with  $L = 7$ ,  $L_A = 3$ ,  $J = 1$ ,  $\Delta = 0.95$ , and  $h^x = h_z = 0.2$ . (c)  $|c(O)|$  for a two-body term (that does not appear in  $H_A$ ) in  $H_A^*$  versus  $\beta$ , for the same parameters as (a) and (b) but with  $L = 6$  and  $L_A = 4$ .

with distance  $d > 1$  and one-body operators with  $d \geq 1$  should have  $c_k(O) = 0$  for  $k = 1, 2$ . These operators are not the identity. But  $H_{A,1}^* \propto \mathbb{1}_A$  by Eq. (10), when  $H_{AB}$  contains no mixed Pauli operators, so  $c_1(O) = 0$ . In Ref. [52] we show how  $c_2(O) = 0$  follows from Eq. (11). For  $k > 2$ ,  $H_{A,k}^*$  becomes intractable to calculate. However, we can formulate a heuristic argument for Eq. (12), based on the following:

*Conjecture.* We express the operator  $O$  in terms of tuples  $h_1, \dots, h_{k+1}$  up to a constant  $O \equiv h_1 \cdots h_{k+1}$  ( $k \geq 1$ ), where the  $h_i$  are all in  $H$ . If all such tuples  $h_1, \dots, h_{k+1}$  can be split into two sets of operators  $\mathcal{H}_1 \neq \emptyset$  and  $\mathcal{H}_2$ , such that operators in  $\mathcal{H}_1$  commute with operators in  $\mathcal{H}_2$  and operators in  $\mathcal{H}_1$  have no support in  $B$ , then  $c_k(O) = 0$ .

The conjecture is supported by the  $k = 1$  and  $k = 2$  cases, which follow from Eqs. (10) and (11) [52].

As shown visually in Fig. 3(c), the smallest  $k$  such that there exists a string  $h_1 \dots h_{k+1} \equiv O$ , which cannot be separated into  $\mathcal{H}_{1,2}$ , is given by  $k = 2d$  for nearest-neighbor two-body operators  $O = \sigma_j^x \sigma_{j+1}^x$  and  $k = 2d + 1$  for single-body operators  $O$  and mixed nearest-neighbor two-body operators  $O = \sigma_j^\alpha \sigma_{j+1}^{\alpha'}$  with  $\alpha \neq \alpha'$ . These strings are given by nearest-neighbor two-body operators appearing in  $H$  connecting the bath to the support of the operator  $O$ . We sketch such strings in Fig. 3(c) for  $O = \sigma_j^x \sigma_{j+1}^x$ ,  $O = \sigma_j^y \sigma_{j+1}^y$ , and  $O = \sigma_j^x$ .

The first row of Fig. 3(c) corresponds to representations of  $O = \sigma_j^x \sigma_{j+1}^x$  of the form

$$\sigma_j^x \sigma_{j+1}^x \equiv \sigma_j^x \sigma_{j+1}^x (\sigma_{j+1}^y \sigma_{j+2}^y)^2 \cdots (\sigma_{L_A}^{(x/y)} \sigma_{L_A+1}^{(x/y)})^2 \quad (15)$$

or permutations thereof. Using squares of pairs requires the least number of Pauli operators that connect to the bath while yielding the identity operator. The square structure in Eq. (15), reflected in the double rectangles in Fig. 3(c), provides a visual interpretation of the factor 2 in the lower bound, Eq. (12).

The strings for  $O = \sigma_j^y \sigma_j^x$  and  $O = \sigma_j^x$ , also presented in Fig. 3(c) are similar. They differ only by the first term on the right-hand side in Eq. (15), namely  $\sigma_j^y \sigma_{j+1}^x \equiv \sigma_j^z \sigma_j^x \sigma_{j+1}^x$  and  $\sigma_j^x \equiv \sigma_{j+1}^x \sigma_j^x \sigma_{j+1}^x$ . This agrees with our result that single-body and mixed two-body terms only appear in the HMF when magnetic fields are present in  $H$  [52].

For nearest-neighbor two-body operators  $\sigma_j^\alpha \sigma_{j+1}^{\alpha'}$ , any Pauli string  $h_1 \dots h_{k+1}$  representing the operator with  $k < 2d$  can be separated into sets  $\mathcal{H}_{1,2}$ , because there are not enough operators to construct structures of the type shown in Fig. 3(c). Similarly, for  $k < 2d + 1$  this holds for single-body operators and nearest-neighbor two-body operators  $\sigma_j^\alpha \sigma_{j+1}^{\alpha'}$  with  $\alpha \neq \alpha'$ .

## V. LARGE $\beta$

In the limit  $\beta \rightarrow \infty$ ,  $e^{-\beta H}/Z$  converges to the projector  $P_{GS} = |\Psi_{GS}\rangle\langle\Psi_{GS}|$  onto the ground-state subspace, where  $|\Psi_{GS}\rangle$  is the ground-state wave function of the entire  $(A + B)$  system. The reduced projector

$$\rho_A^{GS} = \text{tr}_B(P_{GS}) = \text{tr}_B(|\Psi_{GS}\rangle\langle\Psi_{GS}|), \quad (16)$$

i.e., the reduced density matrix of the  $A$  region in the ground-state wave function, is a widely studied object, as it encodes the entanglement between  $A$  and  $B$ . It is often expressed in



terms of an “effective” Hamiltonian  $\mathcal{H}_A^E$ , the entanglement Hamiltonian [42–45]:

$$e^{-\mathcal{H}_A^E} = \rho_A^{GS} = \lim_{\beta \rightarrow \infty} \text{tr}_B(e^{-\beta H}) Z^{-1}. \quad (17)$$

Comparing with Eq. (1), we obtain the following relationship for  $\beta \gg 1$  between the HMF  $H_A^*$  and the entanglement Hamiltonian  $\mathcal{H}_A^E$ :

$$\mathcal{H}_A^E \approx \beta H_A^* + \ln(Z^*). \quad (18)$$

In other words, the entanglement Hamiltonian is obtained by shifting and scaling the HMF at large  $\beta$ . This relation extends the previously derived result that  $H_A^* \propto \mathbb{1}_A$  in the same limit [13].

The shifted and scaled operator  $\tilde{H}_A^* = \beta H_A^* + \ln(Z^*)$  is compared in Fig. 4(b) to  $\mathcal{H}_A^E$  for  $\beta \gg 1$  limit. As predicted, the distance between the two “Hamiltonians” vanishes for  $\beta \rightarrow \infty$ .

## VI. CONCLUDING DISCUSSION

In this work, we investigated the (spatial) structure of the HMF, a fundamental concept in understanding the implications of nonweak coupling in thermodynamics. We demonstrated and explained a skin effect in the HMF structure: The magnitude of terms in  $H_A^* - H_A$  decreases exponentially with the distance from the boundary. We also identified the types of terms that can appear in the HMF and at which order they can occur.

The idea of a skin effect in the deviation of the HMF from the system Hamiltonian is related in spirit to ideas discussed in the literature around locality of temperature [53–56]. Since thermal states of systems described by short-range interactions incorporate a notion of locality, it makes sense that the effect on the HMF should be localized near the boundary. To the best of our knowledge, one cannot infer the explicit exponential behavior, Eqs. (5) and (6), from such intuition alone.

While our explicit examples and expressions are for a spin- $\frac{1}{2}$  chain with one-body and nearest-neighbor two-body terms and for traceless operators, it is clear that analogous expressions can be worked out for other cases (fermions, bosons,

spins  $> \frac{1}{2}$ , other local operators, other geometries), and that the physical conclusions are generic.

The form of the skin effect and the skin depth, Eqs. (5) and (6), do not depend on the strength of the “system-bath” coupling  $H_{AB}$ . We see from the perturbative construction that the coupling strength can affect the coefficient at most polynomially in  $d$ , leaving the exponential decay in Eq. (6) and hence the length  $d_c$  unaffected. We have also explicitly tested this independence numerically [52].

Our perturbative construction, and the arguments leading to the skin effect, do not require the subsystem  $B$  to be large. Thus, the results are independent of “bath size” in the sense that the form  $|c(O)| \sim e^{-d/d_c}$  of Eq. (5), and the value of  $d_c$ , are not affected by the size  $L_B$  of the  $B$  partition [52]. Changing  $L_B$  does affect the prefactor in Eq. (5), i.e., the magnitude of  $|c(O)|$ .

In addition, the chaotic vs integrable nature of the Hamiltonian, although generally important for thermalization/thermodynamics, plays no role, and our results are independent of integrability.

Our results open up several research directions. (i) The skin-effect structure is based on locality; one might ask whether some version of this picture survives for long-ranged Hamiltonians with power-law decay of couplings. (ii) Notions of boundary locality have been discussed for the entanglement Hamiltonian and its spectrum [45,57,58]. It is intriguing to ask whether these might be related to the skin effect we have presented for the HMF. (iii) Numerically, we found the constant  $a$  in Eq. (6) to be relatively large ( $>1$ ), leading to a rather sharp skin effect (small  $d_c$ ); the deviations of  $H_A^*$  from  $H_A$  are strongly localized near the boundary. Whether this is a generic feature for different classes of systems remains an open question. (iv) In this work we have focused on the exponential behavior  $|c(O)| \sim e^{-d/d_c}$  and on the constant  $d_c$ , and have not attempted to treat the prefactor, i.e., the absolute magnitude of  $|c(O)|$ , explicitly. For example, the way this prefactor depends on the size of the  $B$  partition remains an open question.

## ACKNOWLEDGMENTS

P.C.B. acknowledges funding from Science Foundation Ireland through Grant No. 21/RP-2TF/10019. This work was in part supported by the Deutsche Forschungsgemeinschaft under Grant No. SFB 1143 (Project No. 247310070).

- [1] F. Binder, L. A. Correa, C. Gogolin, J. Anders, and G. Adesso, 1st ed., *Thermodynamics in the Quantum Regime* (Springer International Publishing, Cham, Switzerland, 2018).
- [2] M. Campisi, P. Talkner, and P. Hänggi, Fluctuation theorem for arbitrary open quantum systems, *Phys. Rev. Lett.* **102**, 210401 (2009).
- [3] P. Talkner and P. Hänggi, *Colloquium*: Statistical mechanics and thermodynamics at strong coupling: Quantum and classical, *Rev. Mod. Phys.* **92**, 041002 (2020).
- [4] J. G. Kirkwood, Statistical mechanics of fluid mixtures, *J. Chem. Phys.* **3**, 300 (1935).

- [5] C. Jarzynski, Nonequilibrium work theorem for a system strongly coupled to a thermal environment, *J. Stat. Mech.* (2004) P09005.
- [6] M. E. Tuckerman, *Statistical Mechanics: Theory and Molecular Simulation* (Oxford University Press, New York, USA, 2010).
- [7] M. F. Gelin and M. Thoss, Thermodynamics of a subensemble of a canonical ensemble, *Phys. Rev. E* **79**, 051121 (2009).
- [8] S. Hilt, B. Thomas, and E. Lutz, Hamiltonian of mean force for damped quantum systems, *Phys. Rev. E* **84**, 031110 (2011).
- [9] R. Gallego, A. Riera, and J. Eisert, Thermal machines beyond the weak coupling regime, *New J. Phys.* **16**, 125009 (2014).

- [10] A. Rivas, Strong coupling thermodynamics of open quantum systems, *Phys. Rev. Lett.* **124**, 160601 (2020).
- [11] J. D. Cresser and J. Anders, Weak and ultrastrong coupling limits of the quantum mean force Gibbs state, *Phys. Rev. Lett.* **127**, 250601 (2021).
- [12] Y.-F. Chiu, A. Strathearn, and J. Keeling, Numerical evaluation and robustness of the quantum mean-force Gibbs state, *Phys. Rev. A* **106**, 012204 (2022).
- [13] T. Chen and Y.-C. Cheng, Numerical computation of the equilibrium-reduced density matrix for strongly coupled open quantum systems, *J. Chem. Phys.* **157**, 064106 (2022).
- [14] A. E. Teretenkov, Effective Gibbs state for averaged observables, *Entropy* **24**, 1144 (2022).
- [15] A. S. Trushechkin, M. Merkli, J. D. Cresser, and J. Anders, Open quantum system dynamics and the mean force Gibbs state, *AVS Quantum Science* **4**, 012301 (2022).
- [16] G. M. Timofeev and A. S. Trushechkin, Hamiltonian of mean force in the weak-coupling and high-temperature approximations and refined quantum master equations, *Int. J. Mod. Phys. A* **37**, 2243021 (2022).
- [17] J. S. Lee and J. Yeo, Perturbative steady states of completely positive quantum master equations, *Phys. Rev. E* **106**, 054145 (2022).
- [18] N. Anto-Sztrikacs, A. Nazir, and D. Segal, Effective-Hamiltonian theory of open quantum systems at strong coupling, *PRX Quantum* **4**, 020307 (2023).
- [19] L. D'Alessio, Y. Kafri, A. Polkovnikov, and M. Rigol, From quantum chaos and eigenstate thermalization to statistical mechanics and thermodynamics, *Adv. Phys.* **65**, 239 (2016).
- [20] R. Nandkishore and D. A. Huse, Many-body localization and thermalization in quantum statistical mechanics, *Annu. Rev. Condens. Matter Phys.* **6**, 15 (2015).
- [21] M. P. Müller, E. Adlam, L. Masanes, and N. Wiebe, Thermalization and canonical typicality in translation-invariant quantum lattice systems, *Commun. Math. Phys.* **340**, 499 (2015).
- [22] A. M. Kaufman, M. E. Tai, A. Lukin, M. Rispoli, R. Schittko, P. M. Preiss, and M. Greiner, Quantum thermalization through entanglement in an isolated many-body system, *Science* **353**, 794 (2016).
- [23] A. Dymarsky, N. Lashkari, and H. Liu, Subsystem eigenstate thermalization hypothesis, *Phys. Rev. E* **97**, 012140 (2018).
- [24] J. R. Garrison and T. Grover, Does a single eigenstate encode the full Hamiltonian? *Phys. Rev. X* **8**, 021026 (2018).
- [25] P. C. Burke, G. Nakerst, and M. Haque, Assigning temperatures to eigenstates, *Phys. Rev. E* **107**, 024102 (2023).
- [26] M. Rigol, V. Dunjko, and M. Olshanii, Thermalization and its mechanism for generic isolated quantum systems, *Nature (London)* **452**, 854 (2008).
- [27] M. Rigol, Breakdown of thermalization in finite one-dimensional systems, *Phys. Rev. Lett.* **103**, 100403 (2009).
- [28] M. Rigol, Quantum quenches and thermalization in one-dimensional fermionic systems, *Phys. Rev. A* **80**, 053607 (2009).
- [29] M. Rigol and L. F. Santos, Quantum chaos and thermalization in gapped systems, *Phys. Rev. A* **82**, 011604(R) (2010).
- [30] L. F. Santos and M. Rigol, Onset of quantum chaos in one-dimensional bosonic and fermionic systems and its relation to thermalization, *Phys. Rev. E* **81**, 036206 (2010).
- [31] G. Roux, Finite-size effects in global quantum quenches: Examples from free bosons in an harmonic trap and the one-dimensional Bose-Hubbard model, *Phys. Rev. A* **81**, 053604 (2010).
- [32] M. Rigol and M. Srednicki, Alternatives to eigenstate thermalization, *Phys. Rev. Lett.* **108**, 110601 (2012).
- [33] L. F. Santos, A. Polkovnikov, and M. Rigol, Weak and strong typicality in quantum systems, *Phys. Rev. E* **86**, 010102(R) (2012).
- [34] C. Neuenhahn and F. Marquardt, Thermalization of interacting fermions and delocalization in Fock space, *Phys. Rev. E* **85**, 060101(R) (2012).
- [35] E. Khatami, G. Pupillo, M. Srednicki, and M. Rigol, Fluctuation-dissipation theorem in an isolated system of quantum dipolar bosons after a quench, *Phys. Rev. Lett.* **111**, 050403 (2013).
- [36] S. Sorg, L. Vidmar, L. Pollet, and F. Heidrich-Meisner, Relaxation and thermalization in the one-dimensional Bose-Hubbard model: A case study for the interaction quantum quench from the atomic limit, *Phys. Rev. A* **90**, 033606 (2014).
- [37] K. R. Fratus and M. Srednicki, Eigenstate thermalization in systems with spontaneously broken symmetry, *Phys. Rev. E* **92**, 040103(R) (2015).
- [38] F. H. L. Essler and M. Fagotti, Quench dynamics and relaxation in isolated integrable quantum spin chains, *J. Stat. Mech.* (2016) 064002.
- [39] T.-C. Lu and T. Grover, Renyi entropy of chaotic eigenstates, *Phys. Rev. E* **99**, 032111 (2019).
- [40] K. Seki and S. Yunoki, Emergence of a thermal equilibrium in a subsystem of a pure ground state by quantum entanglement, *Phys. Rev. Res.* **2**, 043087 (2020).
- [41] J. D. Noh, Eigenstate thermalization hypothesis and eigenstate-to-eigenstate fluctuations, *Phys. Rev. E* **103**, 012129 (2021).
- [42] H. Li and F. D. M. Haldane, Entanglement spectrum as a generalization of entanglement entropy: Identification of topological order in non-Abelian fractional quantum Hall effect states, *Phys. Rev. Lett.* **101**, 010504 (2008).
- [43] I. Peschel and V. Eisler, Reduced density matrices and entanglement entropy in free lattice models, *J. Phys. A: Math. Theor.* **42**, 504003 (2009).
- [44] V. Eisler and I. Peschel, Properties of the entanglement Hamiltonian for finite free-fermion chains, *J. Stat. Mech.* (2018) 104001.
- [45] M. Dalmonte, V. Eisler, M. Falconi, and B. Vermersch, Entanglement Hamiltonians: From field theory to lattice models and experiments, *Ann. Phys.* **534**, 2200064 (2022).
- [46] P. Strasberg and M. Esposito, Measurability of nonequilibrium thermodynamics in terms of the Hamiltonian of mean force, *Phys. Rev. E* **101**, 050101(R) (2020).
- [47] P. Talkner and P. Hänggi, Comment on "Measurability of nonequilibrium thermodynamics in terms of the Hamiltonian of mean force", *Phys. Rev. E* **102**, 066101 (2020).
- [48] P. Strasberg and M. Esposito, Reply to "Comment on 'Measurability of nonequilibrium thermodynamics in terms of the Hamiltonian of mean force' ", *Phys. Rev. E* **102**, 066102 (2020).
- [49] S. Goldstein, J. L. Lebowitz, R. Tumulka, and N. Zanghì, Canonical typicality, *Phys. Rev. Lett.* **96**, 050403 (2006).
- [50] S. Popescu, A. J. Short, and A. Winter, Entanglement and the foundations of statistical mechanics, *Nat. Phys.* **2**, 754 (2006).
- [51] T. Mori, T. N. Ikeda, E. Kaminishi, and M. Ueda, Thermalization and prethermalization in isolated quantum systems: a

- theoretical overview, *J. Phys. B: At. Mol. Opt. Phys.* **51**, 112001 (2018).
- [52] See Supplemental Materials at <http://link.aps.org/supplemental/10.1103/PhysRevE.110.014111> for detailed derivations of which terms can appear in the HMF and of the small  $\beta$  expansion, in addition to extra numerical data for further  $n$ -body coefficients, for a disordered model, and for tuning the coupling  $J_{AB}$ .
- [53] M. Kliesch, C. Gogolin, M. J. Kastoryano, A. Riera, and J. Eisert, Locality of temperature, *Phys. Rev. X* **4**, 031019 (2014).
- [54] S. Hernández-Santana, A. Riera, K. V. Hovhannisyán, M. Perarnau-Llobet, L. Tagliacozzo, and A. Acín, Locality of temperature in spin chains, *New J. Phys.* **17**, 085007 (2015).
- [55] G. De Palma, A. De Pasquale, and V. Giovannetti, Universal locality of quantum thermal susceptibility, *Phys. Rev. A* **95**, 052115 (2017).
- [56] A. M. Alhambra, Quantum many-body systems in thermal equilibrium, *PRX Quantum* **4**, 040201 (2023).
- [57] V. Alba, M. Haque, and A. M. Läuchli, Boundary-locality and perturbative structure of entanglement spectra in gapped systems, *Phys. Rev. Lett.* **108**, 227201 (2012).
- [58] V. Alba, M. Haque, and A. M. Läuchli, Entanglement spectrum of the two-dimensional Bose-Hubbard model, *Phys. Rev. Lett.* **110**, 260403 (2013).